

Slenderness effects on the simulated response of longitudinal reinforcement in monotonic compression

Luisa María Gil-Martín[†] and Enrique Hernández-Montes[‡]

University of Granada, Campus de Fuentenueva, 18072 Granada, Spain

Mark Aschheim^{††}

Civil Engineering Department, Santa Clara University, 500 El Camino Real, Santa Clara, CA 95053, U.S.A.

Stavroula J. Pantazopoulou^{‡‡}

Department of Civil Engineering, Democritus University of Thrace, Vas. Sofias Street, Xanthi 67100, Greece

(Received April 11, 2005, Accepted March 14, 2006)

Abstract. The influence of reinforcement buckling on the flexural response of reinforced concrete members is studied. The stress-strain response of compression reinforcement is determined computationally using a large-strain finite element model for bars of varied diameter, length, and initial eccentricity, and a mathematical expression is fitted to the simulation results. This relationship is used to represent the response of bars in compression in a moment-curvature analysis of a reinforced concrete cross section. The compression bar may carry more or less force than a tension bar at a corresponding strain, depending on the relative influence of Poisson effects and bar slenderness. Several cross-section analyses indicate that, for the distances between stirrups prescribed in modern concrete codes, the influence of inelastic buckling of the longitudinal reinforcement on the monotonic moment capacity is very small and can be neglected in many circumstances.

Keywords: bars; buckling; models; inelastic action; flexural design; concrete structures.

[†] Associate Professor, Corresponding author, E-mail: mlgil@ugr.es

[‡] Associate Professor, E-mail: emontes@ugr.es

^{††} Associate Professor, E-mail: maschheim@scu.edu

^{‡‡} Professor, E-mail: pantaz@civil.duth.gr

1. Introduction and background

In the moment-curvature analysis of reinforced concrete sections, the contributions of longitudinal reinforcement and concrete to flexural and axial strengths are usually evaluated using the Bernoulli hypothesis that plane sections remain plane. The contribution of the reinforcement is usually established on the basis of a stress-strain relationship. Typically, the stress-strain relationship for tensile behaviour also is assumed to apply to compression behaviour, even though buckling of the compression reinforcement may be anticipated.

Modern simulation tools allow the behaviour of the compression reinforcement to be determined over a large range of deformation with full consideration of instabilities associated with elastic and inelastic material behaviour. Such analyses were not possible at earlier times when seminal advances on buckling were based primarily on theoretical derivation and were hampered by several simplifying assumptions necessitated by the need to obtain closed-form solutions. Contributions by Engesser and Shanley, for example, continue to have great pedagogic value for establishing limit values for cases of buckling in which inelasticity develops.

Buckling is associated with the sudden onset of instability in members under compression. In slender members, elastic buckling occurs when the critical buckling load is reached. In stockier members, the loss of stiffness associated with yielding of the reinforcement causes plastic buckling to occur, regardless of the spacing of stirrups. The buckled shape of the bar is associated with lateral deformation of the bar; a kinematic relation exists between the compressive strain in the bar and the lateral deflection of the buckling bar. When the bar is part of a reinforced concrete member, buckling may or may not occur when conditions of instability are reached, depending on the integrity of the concrete core and the potential for load in the bar to be redistributed to other components of the composite member.

It is well known from classic mechanics solutions that the amplitude of lateral deflection of a buckling member is an indeterminate quantity if the formulation is based on small strain analysis, even when statics are resolved in the deformed configuration. In such studies the buckling load is the load that leads to bifurcation of the classic solution. A more precise analysis requires a large displacement formulation, which adds considerable computational demands to the solution of the problem.

Investigations of a more practical nature, pertaining specifically to inelastic bar buckling in reinforced concrete structures, were carried out with the objective of deriving detailing requirements for design. Bressler and Gilbert (1961) identified a relationship between the critical buckling load of a compressed bar and several design variables such as stirrup spacing, stirrup bar diameter, and stirrup arrangement. They accounted for inelastic buckling by using the tangent steel modulus in the expression for the critical load of an elastic beam-column (Euler's buckling load). A drawback to this approach is that a non-zero tangent modulus need be assumed even for the yield plateau to obtain reasonable estimates of the critical buckling load, as a zero modulus leads to predictions of incipient buckling immediately upon yielding, for bars of any slenderness. To address this inconsistency Papia *et al.* (1988) employed the double modulus concept so as to establish a value for the modulus used in the critical buckling load expression, which is a weighted average of the elastic and tangent moduli. This was meant to account for the stiffness recovery of the bending bar as it buckles, as compressed material unloads as a result of curvature; still, however, the analytical expressions for the double modulus break down when the tangent modulus is zero. To better represent actual behavior, Watson *et al.* (1992) investigated experimentally the influence of bar

slenderness (the ratio of tie spacing to bar diameter) on the strain ductility that may be attained in reinforced concrete members. They defined the tangent steel modulus for the hardening range assuming identical stress-strain responses in tension and compression (in engineering coordinates) in order to determine a critical axial load and corresponding strain ductility as a function of s/D , where s is the distance between two consecutive stirrups and D the bar diameter. No calculations were carried out for the yield plateau. Through calibration with test results, early buckling (i.e., at unacceptably low strain ductility values) was observed to occur for s/D ratios exceeding a value of 8. Based on theoretical argument and calibrations with an extensive database of test results, Pantazopoulou (1998) discussed the redistribution occurring between the concrete core and reinforcement when the bar reaches conditions of instability (i.e., upon yielding). Buckling will occur only when the confined core follows (by collapse) the necessary shortening that the bar needs to undergo in order to buckle. Therefore, occurrence or not of bar buckling in reinforced concrete members will depend upon the integrity of the confined core which supports the reinforcement.

2. Modelling the buckling behaviour of reinforcing bar

Longitudinal reinforcement in reinforced concrete columns contains imperfections, encompassing deviations from straightness or alignment, material imperfections, as well as non-symmetry owing to the pattern of hot-rolled deformations over the bar surface. The bars are supported against lateral deflection by stirrups at discrete locations. However, these supports are not stationary, for compressive forces cause the concrete core to dilate, placing the stirrups in tension, while the longitudinal bar is subjected to bending moments and associated curvatures. The resulting lateral displacements at the bar supports, combined with initial imperfections, induce second-order effects in the longitudinal bars as the compressive force on the bar increases. The state of stress in the adjacent cover is exacerbated further by the lateral expansion of the longitudinal compressed bar due to Poisson effects. Note that owing to Poisson's effects, an isolated steel bar under compression will expand radially by $u = \nu_s \cdot D/2 \cdot \varepsilon_s = 0.15D \cdot \varepsilon_s$, where ε_s the bar axial compressive strain (assuming a ν_s value of 0.3). Thus, upon yielding (e.g., $\varepsilon_s = 0.002$), the bar will displace the cover laterally by as much as $0.0003D$ mm, resulting in a nominal tangential strain at the outside face of the cover equal to $\varepsilon_t = 0.0003D/(C + D/2)$. For usual covers, ($C \approx 2D$), it follows that cover will split near yielding of the bar in compression (e.g., $\varepsilon_{t, split} = f_t'/E_c = 0.00015$, i.e., equal to the rupture strain of concrete in tension). The presence of the reinforcement disturbs the ordinarily complex arrangement of the aggregate particles by aligning them at the surface of the reinforcement, thereby creating a defect in the concrete matrix, while also inducing stress concentrations and reducing the cross sectional area of the cover. Spalling will occur when the split cover separates from the core, thereby exposing the reinforcement. This is followed by buckling of the longitudinal bars because of the loss of lateral restraint to the bars due to loss of cover concrete. For well-confined concrete members these phenomena are bound to occur prior to attainment of the dependable strain capacity of the confined concrete core. Consequently, the solution of the elastic eigenproblem for instability is of little relevance, and a complete plastic buckling analysis generally is required if the response of the bar is to be modelled.

The study of the structural behaviour of reinforced concrete requires models of the constituent materials. Because concrete is a complex composite, empirical evidence is often relied upon to characterize its behavior. Lateral confining pressure is known to have a substantial effect on the

stress-strain behaviour in the principal compressive direction, and several models (e.g., Kent and Park 1971, Mander 1988, Sheikh and Uzumeri 1980) have been proposed in order to represent this effect.

Analysis of the forces and deformations in structures typically is made using discrete beams and columns, as this is more efficient than discretizing the structure into a large number of finite elements for analysis. Simple beam theory (plane sections remain plane) is the basis of the structural analysis and also is used to evaluate the strengths of beam and column cross sections. Depending on its slenderness and strain environment, a longitudinal reinforcing bar under compression may reach the elastic buckling load or the plastic buckling capacity. If the concrete cover is assumed to be ineffective (due to spalling or incipient spalling) then elastic or plastic buckling represents the onset of instability. Beyond the point of instability, buckling will prevail only if development of significant second-order displacements is possible. Because the applied load is shared between the concrete and steel reinforcement, attainment of conditions of instability for the bar signals redistribution of load to concrete, as well as to other (unbuckled) longitudinal bars. Consequently, reinforcement instability does not correspond to sudden failure of the reinforced concrete member, and the load-carrying capacity of the bar prior to and beyond the point of instability must be established to characterize the precise behaviour of the entire cross section.

The objective of this paper is to develop a relationship for the force carried by a reinforcing bar as a function of the average longitudinal strain on the basis of computational simulations of bar buckling in composite cross sections in which material inelasticity, lateral dilation, and transverse restraint is modelled. The derived relationship is used in a flexural sectional analysis in order to evaluate the applicability of conventional analysis assumptions in which a tensile stress-strain relationship is used for the reinforcement in compression.

3. Definition of strain in engineering and natural coordinates

The stress-strain response of steel is characterized by the yield strength, f_y , ultimate strength, f_u , yield strain, ε_y , strain corresponding to the onset of strain hardening, ε_h , and ultimate strain, ε_u . The initial slope of the hardening curve is given by E_h , while the elastic modulus is designated by E . The values of these parameters for a Grade 400 steel are provided in Table 1, in terms of engineering stress and engineering strain. Engineering stress and engineering strain are defined in terms of initial cross sectional area and initial length, respectively.

Rodriguez *et al.* (1999) described the post-yield (hardening) portion of the monotonic curve in tension as

$$f_s = f_u + (f_y - f_u) \left(\frac{\varepsilon_u - \varepsilon_s}{\varepsilon_u - \varepsilon_h} \right)^P \quad (1)$$

$$P = E_h \left(\frac{\varepsilon_u - \varepsilon_h}{f_u - f_y} \right)$$

Table 1 Characteristics of the steel used as longitudinal reinforcement

ε_y	ε_h	ε_u	E_h (MPa)	f_y (MPa)	f_u (MPa)
0.002	0.010	0.120	20000	400	600

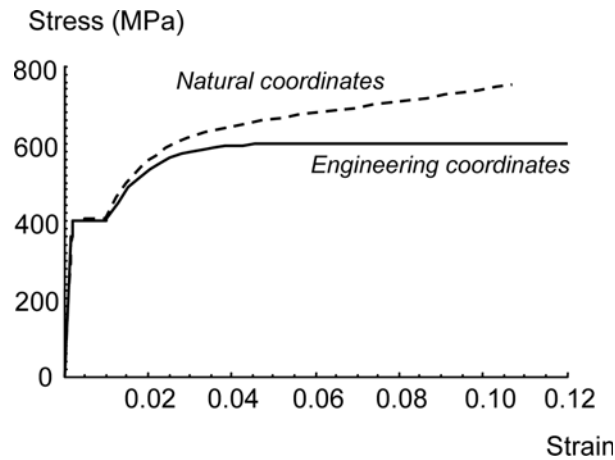


Fig. 1 Stress-strain diagram in tension for the steel grade 400 considered in natural and engineering coordinates

in terms of engineering stress and engineering strain. Because engineering stress and strain are calculated on the basis of the original dimensions, Eq. (1) does not distinguish between compression, which causes an increase in cross-sectional area, and tension, which causes a reduction in cross sectional area. These distinctions become significant after the yield plateau, as illustrated by Rodriguez *et al.* (1999). Logarithmic (natural or Hencky) strains and true (natural or Cauchy) stresses can be used to account for these differences, which become significant at large strains. Dodd and Restrepo (1995) reported a parametric relation between natural and engineering strains and stresses. In terms of the engineering strain, ε_s , and engineering stress, f_s , the natural stress, f_{ns} , and natural strain, ε_{ns} , are given as:

$$\begin{aligned} f_{ns} &= f_s(1 + \varepsilon_s) \\ \varepsilon_{ns} &= \ln(1 + \varepsilon_s) \end{aligned} \quad (2)$$

The stress-strain response in natural coordinates determined using Eq. (2) is illustrated in Fig. 1, on the basis of the engineering stress-strain relation provided in the same figure. The abscissa represents strain (natural or engineering) and the ordinate represents stress (natural or engineering), depending on the curve. In the natural coordinate system, the instantaneous cross-sectional area of the element is used, and thus, the same curve applies to both compression and tension, in the absence of second-order effects.

4. Initial imperfections and transverse deformation

Second-order effects (internal moments resulting from statics in the deformed configuration) occur when the bar deforms transversely, and are present as initial conditions when the bar is not perfectly straight at the beginning of the loading process. Prior work on longitudinal reinforcement buckling addresses transverse deformation in different ways.

Bayrak and Sheikh (2001) conducted experiments to determine the compressive stress carried by longitudinal reinforcing bars prior to and beyond the point of instability. Initial out-of-straightness and bar slenderness were variables in the experiments. The initial deformation was imposed by inducing a rotation at the ends of the bar, which were clamped during testing. Several values of initial deformation were induced in the tests. The experiments showed that the initial out-of-straightness has influence on the maximum force sustained by the bar.

Prior works such as Monti and Nuti (1992) or Mau and El-Mabsout (1987) presented different views about the influence of initial out-of-straightness. Monti and Nuti tested reinforcement coupons in compression. They used an Italian steel with a nominal yield strength of 440 MPa. Although unavoidable, initial imperfections were not an explicit parameter of their tests. Mau and El-Mabsout developed a special beam-column element to study the inelastic post-buckling behaviour of reinforcing bars. In their computational study, initial imperfections were neglected.

In order to evaluate the influence of initial out-of-straightness on the compressive behavior of reinforcing bars and the effect of bar instability on flexural behaviour of reinforced concrete members, a series of nonlinear finite element analyses were conducted in the present work. The magnitude of initial out-of-straightness considered was of the degree prescribed by Eurocode 3 (1993). Deflections calculated by Bayrak and Sheikh (2001) based on imposed end rotations and by consideration of the interaction between the reinforcing cage and core concrete were used as input parameters in the analysis. Deflection values were obtained by processing the experimental results of the tests conducted by Sheikh (1978) on square columns; these deflections were considered to correspond to the onset of bar buckling, i.e., they were thought to represent the initial condition for the bars at the onset of instability.

In reinforced concrete members with modern detailing, spalling of the concrete shell typically occurs at strains well beyond the yield strain of steel reinforcement. The analytical results described in the following and those cited previously indicate that once the bar yields, the degree of initial out-of-straightness has an insignificant effect on the post-yield stress-strain response. Rather, loss of lateral restraint associated with spalling of the cover concrete is a much more significant event. This observation indicates that lateral dilation of the concrete is not likely to have a significant effect, for the lateral displacement it causes is of similar magnitude as commonly encountered initial out-of-straightness.

5. Framework of study

In order to determine the flexural strength of a cross section as a function of its curvature, it is necessary to represent the force carried by the bar in terms that are relevant to sectional analyses. Thus, in order to characterize the stress-strain behavior of longitudinal reinforcing bars in compression, three-dimensional finite element models of reinforcing bars in compression were developed. The nonlinear step-by-step analyses were performed using the ANSYS (2004) finite element package and considered large-strain effects. The models represented different degrees of initial out-of-straightness for fairly common combinations of bar size and stirrup spacing: bar diameters of 16, 20 and 25 mm and unsupported lengths (i.e., distance between successive stirrups) of 100, 150, 200 and 300 mm were considered. Because no guidelines for initial out-of-straightness in steel reinforcement are available, the criteria specified in Eurocode 3 for structural steel members were used. A circular cross section of the bar was modelled; hot-rolled deformations, which vary

with manufacturer, were not represented. Load-displacement responses were computed using ANSYS.

An *equivalent* stress-strain response for steel in compression was determined, intended for use in the sectional moment-curvature analysis of reinforced concrete members. The equivalent stress-strain response is defined in engineering coordinates; the axial strain in the bar is defined as the axial shortening of the bar divided by the spacing of the transverse reinforcement in the undeformed configuration. Therefore, compatibility between deformations of concrete and reinforcement is maintained in the analyses in longitudinal direction at the scale of the transverse reinforcement spacing. In the following, the stress-strain response in engineering coordinates is used to quantify the influence of bar slenderness and initial bar out-of-straightness.

6. Analytical modelling

The analytical model comprised three-dimensional solid finite elements representing the longitudinal bar and the restraint provided by transverse hoops at a spacing s . Only the bar segment between adjacent hoops was modelled. As previously discussed, lateral deformations of the dilating concrete are likely to be of minor significance, and hence the concrete was not modelled. The ends of the bar segment were restrained from rotation, and loading was achieved by moving the nodes at one end of the model uniformly towards the other end (by displacement control).

Grade 400 steel was modelled using the parameters of Table 1 and a Poisson ratio of 0.3. For the plastic behaviour of steel a multi-linear kinematic hardening model was used. The Solid-92 element within the ANSYS (2004) package was used throughout the model. This element is defined by ten nodes, each having three degrees of freedom consisting of translations in the global x , y and z directions. This element also has plasticity, stress stiffening, large deflection and large strain capabilities. The steel stress-strain response used is given in Fig. 1, with respect to both natural and engineering coordinates. The number of elements used ranged from 201 to 453 for span lengths of 100 to 300 mm.

7. Influence of initial out-of-straightness

The first part of the study addresses the influence of initial out-of-straightness. A 20-mm diameter bar having varied lengths was analyzed (see Fig. 2). Initial out-of-straightness was modeled by an initial lateral displacement at the middle of the span. Two approaches were taken to represent the initial out-of-straightness. In the first approach, the initial geometry of the bar was altered without inducing stress to represent the initial out-of-straightness. In the second approach, an initially straight bar was deformed laterally by the amount of the initial imperfection by imposing a lateral force at the midspan nodes, thereby inducing stress. The initial out-of-straightness is parameterized by the midspan displacement or eccentricity. Two values of initial eccentricity were considered for each bar, indicated in Fig. 2. For each bar, the smaller value is the value prescribed by Eurocode 3 (1993), and the larger initial imperfection corresponds to the deflection calculated by Bayrak and Sheikh (2001) that initiates buckling of the longitudinal bar. The initial imperfection prescribed by Eurocode 3 is found to result in an equivalent stress-strain curve that is similar to the equivalent stress-strain curve obtained using the deflections calculated by Bayrak, as may be seen in Fig. 2 for

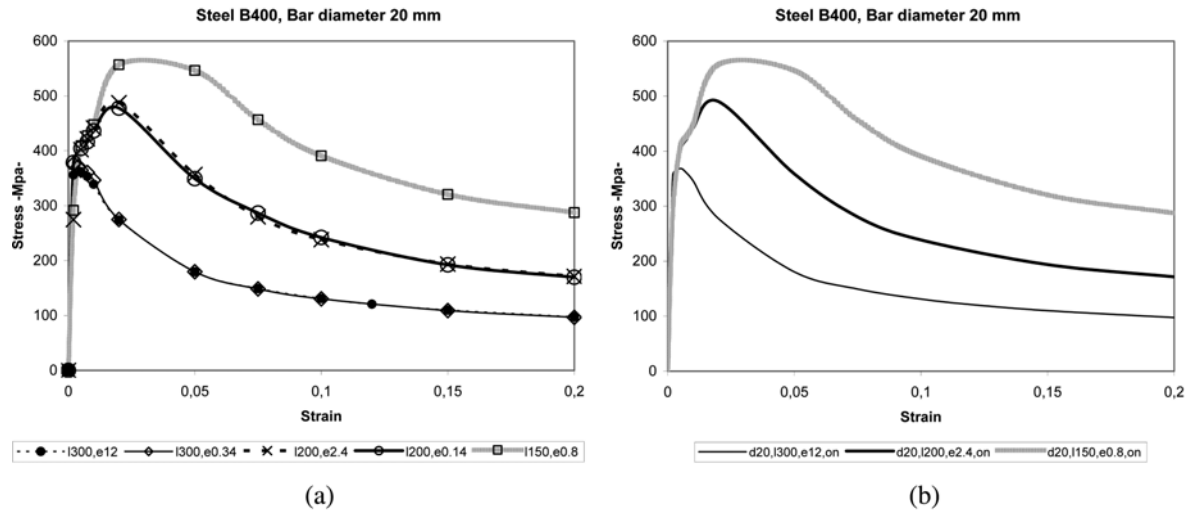


Fig. 2 Compression stress-strain curve in engineering coordinates for a 20 mm-diameter bar with different initial imperfections and various alternative distances between stirrups. A. Initial deformation considered. B Initial deformation not considered.

a 20-mm diameter bar. Thus, initial out-of-straightness has a negligible influence on response.

Because initial out-of-straightness has a very small effect on the equivalent stress-strain response of the bar (Fig. 2) for all strain levels, lateral deformations associated with the dilation of the core concrete, and the lateral forces this may impose on the longitudinal bar, are of reduced significance. For this reason, the core concrete was not explicitly represented in the finite element model.

8. Comparison of tensile and laterally-supported compressive behaviour

To address the common use of the tensile stress-strain behavior as representative of the compressive response in practical flexural analysis, a laterally supported bar was loaded monotonically in tension or compression. Because the analytical model uses a large-strain formulation, the results in tension and compression differ, even in the absence of buckling. Fig. 3 depicts the simulated tensile and compressive response for a 25-mm diameter bar having a length of 100 mm. This bar was laterally supported along its entire length by restraining the lateral displacement along the axis of the bar. For compression loading, two cases were considered. In the first case the bar was perfectly straight. In the second, an initial out-of-straightness was modelled with altered geometry of the bar. The results, plotted in Fig. 3 in terms of engineering stress and strain, indicate that the bar with no eccentricity strain hardens, ultimately developing a larger force than the tension bar, while the bar with initial eccentricity yields at a lower stress, but the stress approaches that of the bar with no eccentricity as strains increase further. The bar with initial eccentricity displays a sloped yield plateau.

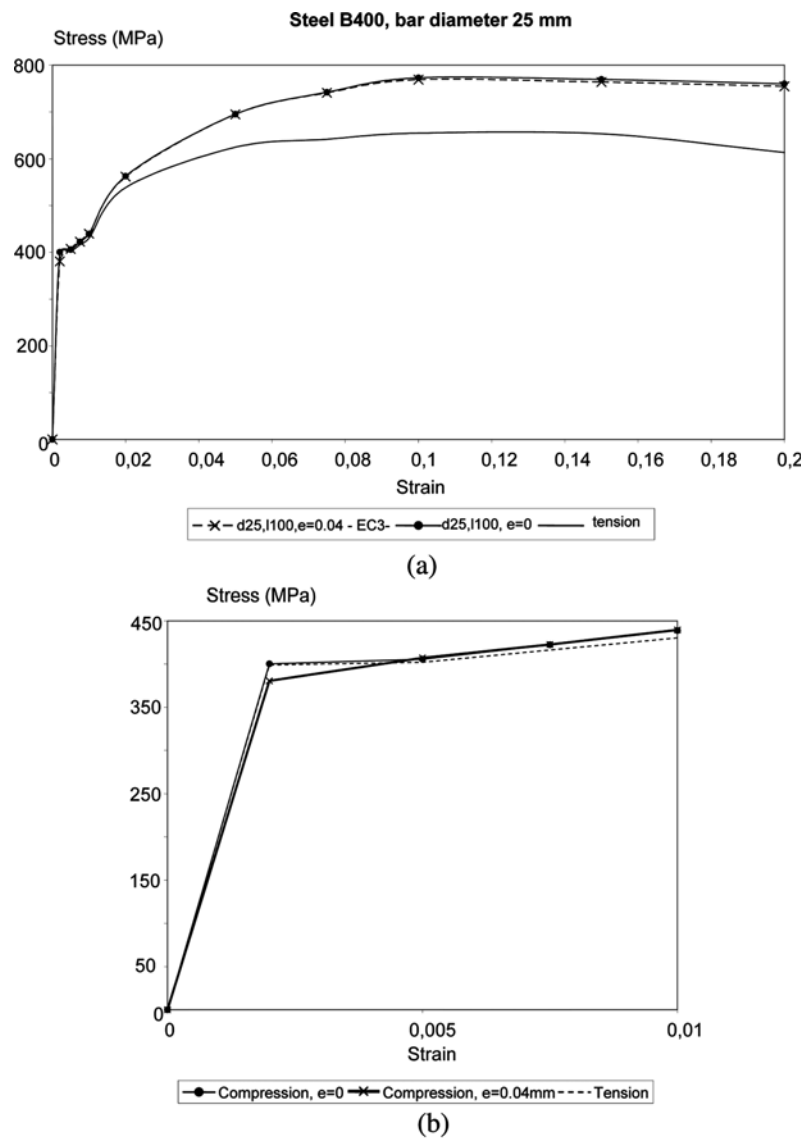


Fig. 3(a) Stress-strain diagram for a laterally-braced Grade 400 bar, under tension and compression, in engineering coordinates, (b) Detail of the yield plateau zone for tension and compression

9. Simulation results for monotonic compression of laterally unsupported bars

Fig. 2, used previously to show that the stress owing to an imposed initial eccentricity or out-of-straightness may be neglected if the objective is to capture buckling response, is now used to illustrate the effects of different values of initial eccentricity and stirrup spacing (or slenderness) for a 20-mm diameter reinforcing bar. Initial out-of-straightness is seen to have a relatively minor effect on the resulting stress-strain behaviour of the bar; the dominant effect is due to the spacing of the stirrups. Therefore, in the remainder of the parametric investigation, a reasonable hypothesis is to

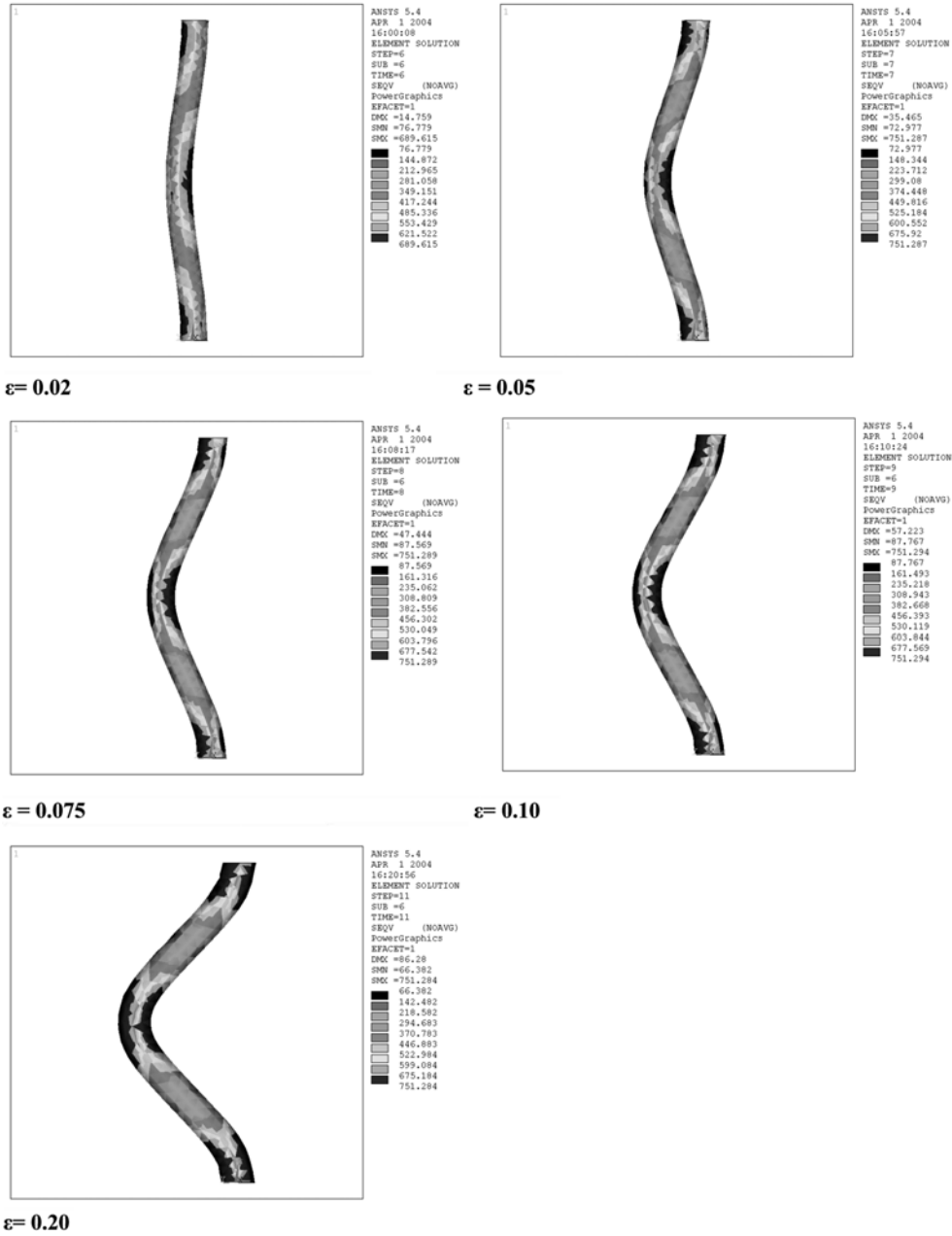


Fig. 4(a) Deformed shape and von Mises stress distribution for a longitudinal bar of 25 mm diameter and length of 300 mm

use a single value for the initial imperfection such as specified by Eurocode 3, while considering the slenderness of the bar as a variable.

Figs. 4(a) and 4(b) illustrate the deformed shape and the von Mises stress distribution for a 25-mm diameter bar for stirrup spacings of 300 and 100 mm, respectively. Fig. 4 reflects the influence of

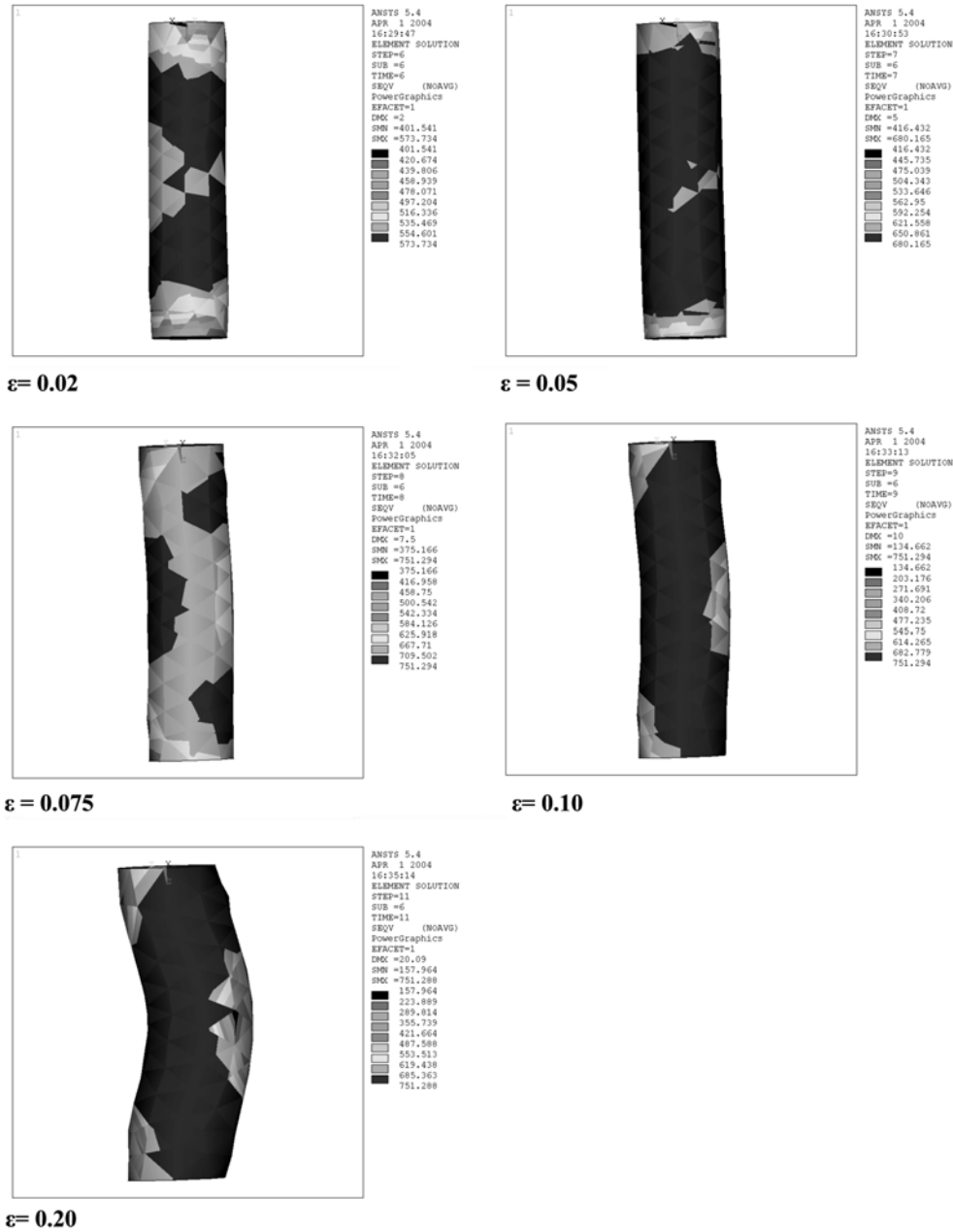


Fig. 4(b) Deformed shape and von Mises stress distribution for a longitudinal bar of 25 mm diameter and length of 100 mm

plasticity and the distribution of the plastic zone on the deformed shape of the bar. The deformed shapes are observed to change as the amplitude of the transverse deformation grows. Curves are fitted to the simulation results rather than using a simple shape function in an analytical formulation for inelastic buckling. Rodriguez *et al.* (1999) among others demonstrated that, for reinforcing bars

tested under monotonic compression, initial eccentricity can cause the yield plateau to have a positive slope in plots of engineering stress versus engineering strain. This effect is also apparent in the numerical results of Fig. 2, for stirrup spacings of 150 and 200 mm. Fig. 3(b) illustrates this point using a close-up view of the response through the yield plateau. Therefore, for fully-supported bars, it is not so much Poisson effects that cause the yield plateau to have a positive slope; rather, this phenomenon is due to initial out-of-straightness. The yield plateaus in Fig. 2 also have a nonzero slope, with a positive slope resulting for the stockier bars and a negative slope resulting for the more slender bars. An initial eccentricity is present for all bars plotted in Fig. 2.

10. Data regression for monotonic compression

A mathematical expression was fitted to the simulated stress-strain responses, with coefficients evaluated for different conditions of bar diameter and hoop spacing. Several mathematical forms were considered, and the general expression given by Eq. (3), having five parameters, was selected.

$$\sigma(\varepsilon) = \begin{cases} E_s \cdot \varepsilon & \text{if } \varepsilon \leq 0.95 \cdot \varepsilon_y \\ 100 \left[a + b \cdot 10^{c \cdot \varepsilon} + \frac{d}{1 + e \cdot \varepsilon^2} \right] & \text{if } 0.95 \cdot \varepsilon_y < \varepsilon \leq 0.12 \end{cases} \quad (3)$$

The pondered least squares technique (Isaacson and Keller 1994) was used to determine the five coefficients for stress-strain curves representing different bar diameters and for different hoop spacings. These coefficients a , b , c , d , and e assume the values given in Table 2, for a Grade 400 steel having the properties of Table 1. The values of Table 2 are given as a function of the bar slenderness, L/D , where L = the spacing of the stirrups and D = the diameter of the longitudinal bar. Fig. 5 compares the results of the simulation with Eq. (3) for the 16-mm and 25-mm bars. The same approach can be used to derive values of the parameters a , b , c , d , and e for steels with other properties.

For values of L/D between those tabulated in Table 2, linear interpolation may be used for the variables b to e , whereas a parabolic interpolation is recommended for the variable a together with the constraint $\sigma(0.95 \cdot \varepsilon_y) = 0.95 \cdot f_y$ N/mm². This interpolation procedure was used to produce the stress-strain curves of Fig. 6 for a Grade 400 steel for five values of slenderness (L/D).

Variations of the parameters a to e are plotted in Fig. 7 as function of L/D . The constants display a sensitivity to slenderness for values of L/D between 5 and 10 or 11, consistent with previous findings (Mau and El-Mabsont 1987).

Table 2 Coefficient values (Eq. (3)) for steel grade 400 with the stress-strain characteristics given in Table 1

L/D	4	5	6	7.5	8	10	12	15	18.75
a	10.46	7.53	4.37	1.74	1.62	1.25	1.14	0.98	0.59
b	-25.00	-23.46	-19.69	-11.58	-9.12	-5.76	-2.16	0.55	2.78
c	-1.85	-2.15	-2.74	-6.00	-6.50	-9.42	-15.85	-35.71	-48.33
d	18.14	19.51	18.88	13.35	11.04	8.08	4.69	2.36	0.95
e	30.50	41.21	61.05	107.33	206.19	352.28	816.85	790.63	237.25

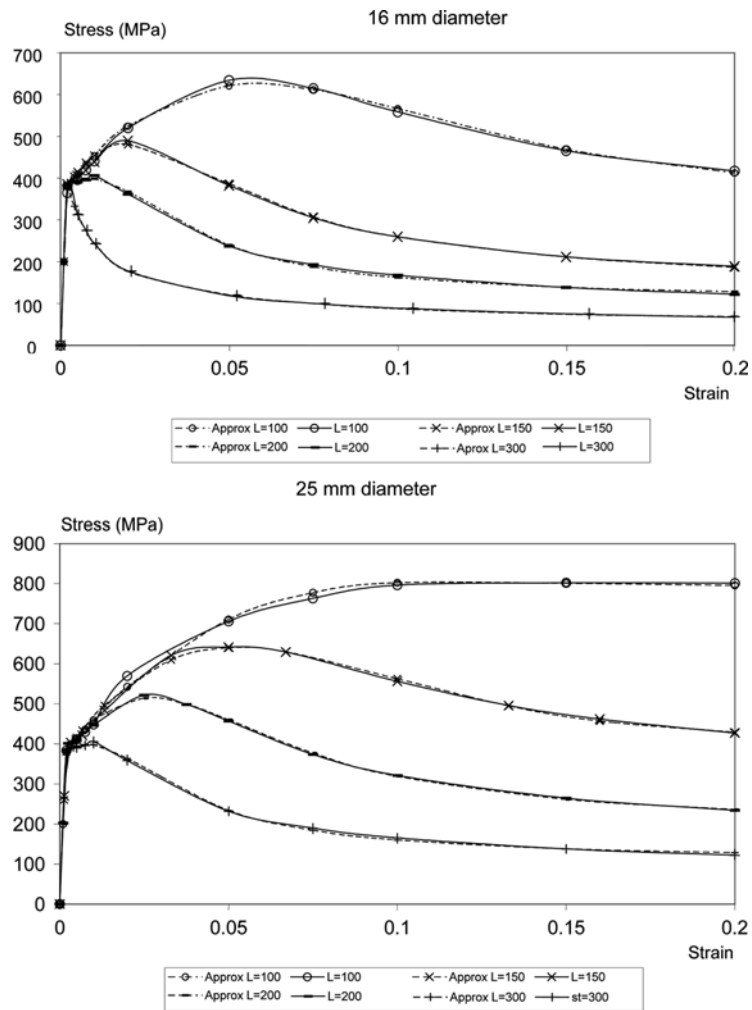


Fig. 5 FEM data and approximated expression for 16 mm and 25 mm diameter bars. L = distance between consecutive stirrups

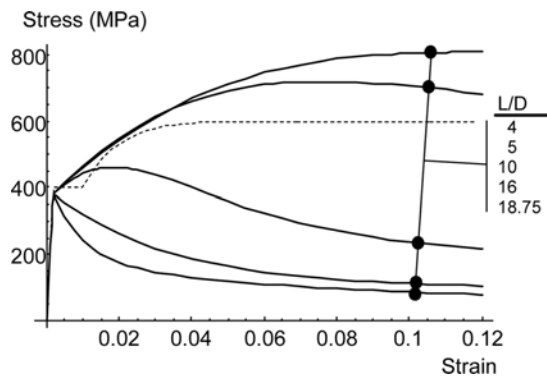


Fig. 6 Analytical model for several L/D values. The dashed line represents the tensile stress-strain curve in engineering coordinates.

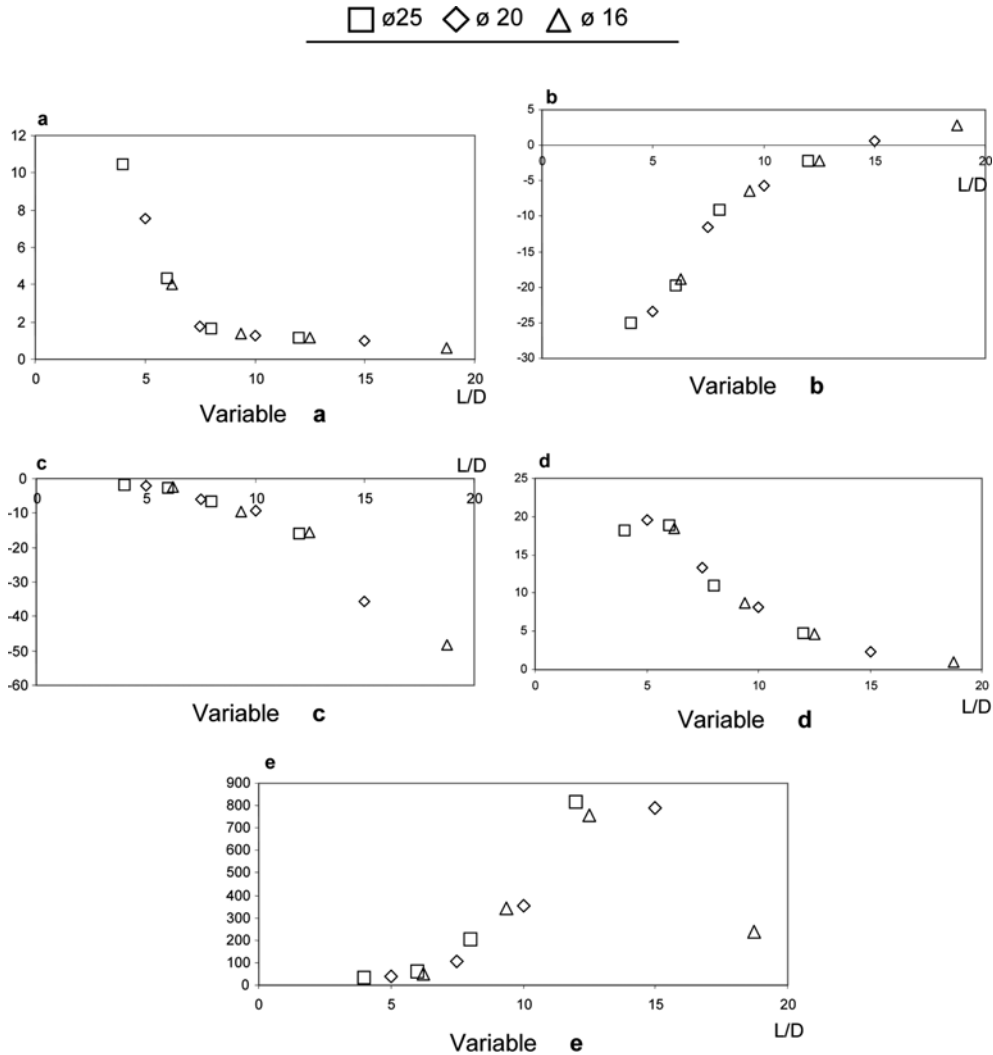


Fig. 7 Variation of the constants in the approximate expression (Eq. (3))

11. Application to moment-curvature analysis

As previously stated, moment-curvature analysis typically is carried out using a stress-strain relationship expressed in terms of engineering stress and engineering strain, developed for bars in tension, but applied to both compression and tension reinforcement (e.g., Wallace and Moehle 1989). The effect of using a compression stress-strain curve for the compression bars modified to account for buckling, in conjunction with a tension stress-strain curve for the tension bars, is determined in this section for an example cross section.

The 500-mm square reinforced concrete column cross section of Fig. 8 was designed in accordance with Eurocode-2 (1991), for a C25/30 concrete, having a characteristic cylinder strength (f_{ck}) equal to 25 MPa and characteristic steel strength (f_{yk}) of 400 MPa. Longitudinal reinforcement

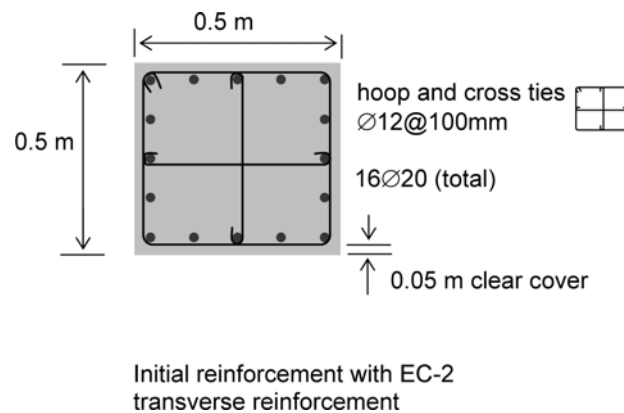


Fig. 8 0.5 m square reinforced-concrete column cross section

consists of $16\text{Ø}20$ bars (20-mm diameter) distributed symmetrically around the perimeter of the cross section. This amount of reinforcement corresponds to a reinforcement ratio of 2% (with respect the gross sectional area), representative of sections commonly used in practice. Transverse steel, consisting of hoops and ties of 12-mm diameter are spaced at 100 mm along the length of the column.

To clearly identify the effect of accurately modelling the compressive stress-strain behaviour of the bars, moment curvature analyses were conducted on a cross section having only top and bottom reinforcement. The top and bottom reinforcement consist of $5\text{Ø}20$ bars at each location. The intermediate bars of Fig. 8, which are absent from the section subjected to moment curvature analyses, would behave similarly for both approaches to modelling the compressive behaviour, and thus their inclusion would reduce any apparent differences in the computed response of the cross section. The cover concrete is included in the moment-curvature analysis, but because it is unconfined, it becomes ineffective soon after the compressive strength is attained. The core concrete continues to carry stress at high strains. These phenomena are modelled in the moment-curvature analyses using the confined concrete stress-strain model by Mander *et al.* (1988). The moment-curvature analyses were conducted for the cross-section assuming a constant axial load equal to 33 percent of the crushing load capacity (1500 kN).

Fig. 9 shows the stress-strain curves used in the moment-curvature analyses for the steel in tension and compression. The specified transverse reinforcement corresponds to $L/D = 5$. The stress-strain curve for steel in compression was generated using Eq. (3) with the parameter values of Table 2. Due to the increase in cross-sectional area of the bars under compression and the close spacing of transverse reinforcement, the engineering stress-strain curve in compression reaches higher stress levels than for the bars in tension. The enhanced strength allows the section to develop a slightly larger flexural strength compared with the conventional analysis in which the bars are modelled using only the tension stress-strain curves. It may be observed that the value of maximum moment is nearly identical, whether computed using symmetric or unsymmetric stress-strain laws.

The same cross-section, having the same longitudinal reinforcement and axial load, but with the spacing of 12-mm diameter hoops and ties increased to 300 mm (an L/D ratio of 15) was also analysed. Because of instability associated with the large slenderness, the engineering stress levels attainable by the bars in compression are lower than those carried by the bars in tension. The

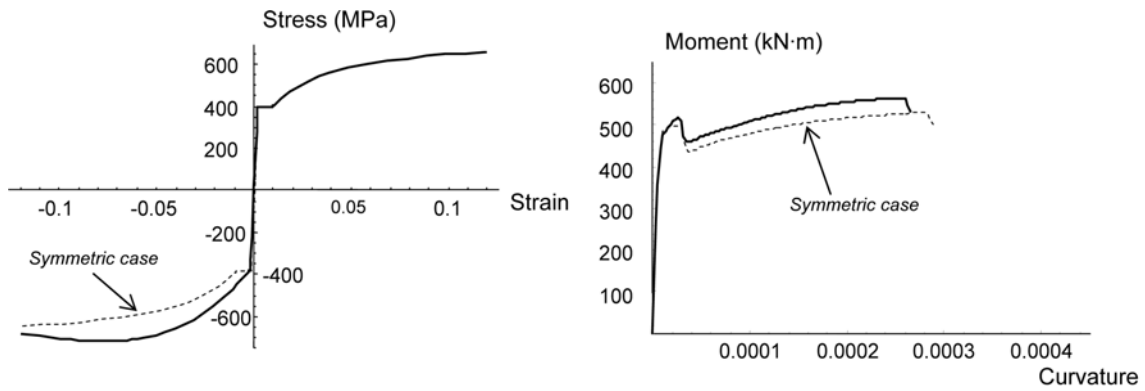


Fig. 9 Derived stress-strain relationship for steel in compression having $L/D = 5$, and corresponding moment curvature diagram for 1500 kN axial load

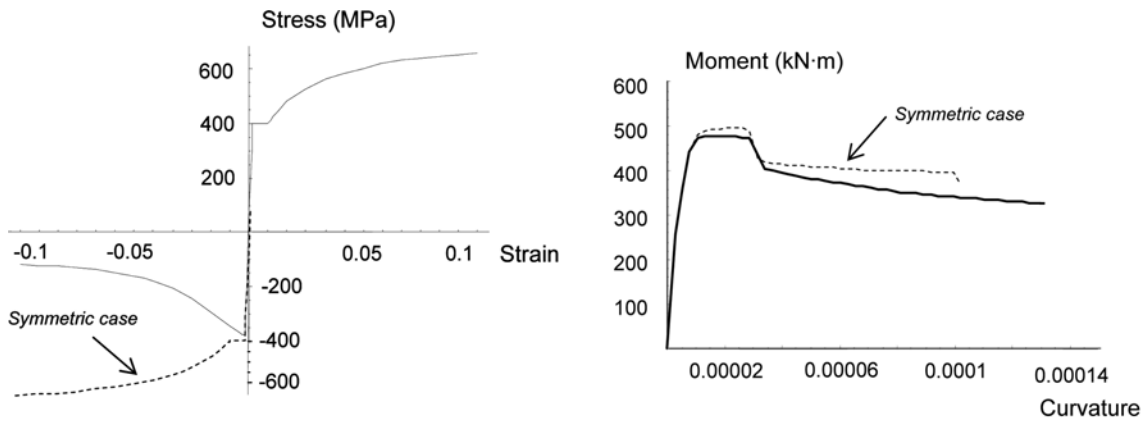


Fig. 10 Derived stress-strain relationship for steel in compression having $L/D = 15$, and corresponding moment curvature diagram for 1500 kN axial load

resulting moment-curvature response is plotted in Fig. 10. It may be observed that buckling of the compression bars results in the section having a slightly smaller flexural strength as compared with the result of conventional analysis.

Clearly, using Eq. (3) to model the compression stress-strain curves of longitudinal reinforcement enables a more precise calculation of flexural strength, as well as the determination of the entire moment-curvature response. However, the effect this has on the estimated flexural strength is relatively small as depicted in Figs. 9 and 10, and therefore it might prove difficult to discern this effect in experimental studies. Based on the present analytical investigation, it appears that flexural strength can be estimated with sufficient accuracy using the conventional approach.

12. Conclusions

A three-dimensional finite element model using large-strain formulation was used to explore the post-yielding behaviour of compression reinforcement with particular emphasis on the effects of bar

slenderness and initial eccentricity on the equivalent stress-strain characteristics of steel bars. Mathematical expressions were fitted to the simulated response in order to characterize the resistance of compression bars in monotonic moment-curvature analyses. It was found that:

1. Bar slenderness has a pronounced effect on the stress carried by the bar at longitudinal strains in excess of the yield strain.
2. Out-of-straightness, whether due to fabrication or distortion of the member cross section, has a relatively small effect on the longitudinal stress carried by the bar at longitudinal strains in excess of the yield strain. The positively sloped yield plateau observed in both experimental and computational studies results primarily from initial out-of-straightness rather than Poisson effects (which were represented explicitly in the large-strain formulation).
3. Although instability causes a reduction in the load-carrying capacity of bars in compression, Poisson effects can result in an increase in the load-carrying capacity of compression bars relative to that of bars in tension. These phenomena result in bars of small slenderness (e.g., $L/D < 5$) having greater force capacity than their tensile counterparts (e.g., Fig. 6), whereas bars having substantially greater slenderness have reduced force capacity relative to their tensile counterparts (e.g., Fig. 6).
4. In moment-curvature analyses, the relative influence of the capacity of the compression bars is reduced by virtue of the substantial compressive capacity of the concrete adjacent to the bar. Consequently, conventional analyses, in which the compressive engineering stress-strain behaviour of the bar is assumed to match the tensile behavior of the bar, provide a reasonable approximation of the flexural strength determined in more precise analyses that account explicitly for buckling of the longitudinal reinforcement.
5. The simulations described herein for one type of steel may be extended to address different types of steels, which may have different characteristics with regard to yield and ultimate strengths, yield plateau, strain hardening stiffness, and ultimate and fracture strains.

Acknowledgments

We extend our sincere appreciation to the Applied Mathematics Department of the University of Granada and especially to Professor Miguel Pasadas for his stimulating discussions on nonlinear regression theories.

References

- Ansys Inc. (2004), Canonsburg, PA 15317. USA. www.ansys.com.
- Bayrak, O. and Sheikh, S. (2001), "Plastic hinge analysis", *J. Struct. Eng.*, ASCE, **127**(9), 1092-1100.
- Bressler, B. and Gilbert, P.H. (1961), "Tie requirements for reinforced concrete columns", *ACI J.*, **58**(26), 555-570.
- Dodd, L.L. and Restrepo-Posada, J.I. (1995), "Model for predicting cyclic behavior of reinforcing steel", *J. Struct. Eng.*, ASCE, **121**(3), 433-445.
- Eurocode 2 (1991), *Design of Concrete Structures. Part 1-1: General Rules and Rules for Buildings*, European Committee for Standardization, Bruxelles, Belgium.
- Eurocode 3 (1993), *Design of Steel Structures. Part 1-1. General Rules and Rules for Building*, European Committee for Standardization, Bruxelles, Belgium.

- Isaacson, E. and Keller, H.B. (1994), *Analysis of Numerical Methods*. Dover Publications.
- Kent, D.C. and Park, R. (1971), "Flexural members with confined concrete", *Proc. ASCE*, **97**(ST7), July, 1969-1990.
- Mander, J.B., Priestley, M.J.N. and Park, R. (1988), "Theoretical stress-strain model for confined concrete", *J. Struct. Eng.*, ASCE, **114**(8), 1804-1826.
- Mau, S.T. and El-Mabsout, M. (1987), "Inelastic buckling of reinforcing bars", *J. Eng. Mech.*, **115**, January 1989.
- Monti, G. and Nuti, C. (1992), "Nonlinear cyclic behavior of reinforcing bars including buckling", *J. Struct. Eng.*, ASCE, **118**(12), 3268-3284.
- Pantazopoulou, S.J. (1998), "Detailing for reinforcement stability in RC members", *J. Struct. Eng.*, ASCE, **124**(6), 623-632.
- Papia, M., Russo, G. and Zingone (1988), "Instability of longitudinal bars in RC columns", *J. Struct. Eng.*, ASCE, **114**(2), 445-461.
- Rodriguez, M.E., Botero, J.C. and Villa, J. (1999), "Cyclic stress-strain behavior of reinforcing steel including effect of buckling", *J. Struct. Eng.*, ASCE, **125**(6), 605-612.
- Sheikh, S.A. (1978), "Effectiveness of rectangular ties as confinement steel in reinforced concrete columns", PhD thesis, University of Toronto, Toronto.
- Sheikh, S.A. and Uzumeri, S.M. (1980), "Strength and ductility of confined concrete columns", *Proc. ASCE*, 1May 1980, **06**(ST5), 1079-1102.
- Wallace, J.W. and Moehle, J.P. (1989), *BIAX: A Computer Program for the Analysis of Reinforced Concrete Sections*, Department of Civil Engineering, University of California, Berkeley, 1989.
- Watson, S., Zahn, F.A. and Park, R. (1992), "Confining reinforcement for concrete columns", *J. Struct. Eng.*, ASCE, **120**(6), 1798-1824.